Electronic Supplementary Material (ESI) for Dalton Transactions.
This journal is © The Royal Society of Chemistry 2017

Supporting Information

Two-way Vapochromism of a Luminescent Platinum(II) Complex with Phosphonic-acid-functionalized Bipyridine Ligand

Atsushi Kobayashi,* Naotaka Yamamoto, Yasuhiro Shigeta, Masaki Yoshida, and Masako Kato*

Department of Chemistry, Faculty of Science, Hokkaido University, North 10 West 8, Kita-ku, Sapporo, Hokkaido 060-0810

Contents

Figure S1. Molecular structures with the numbering schemes of complexes **1P**, **1P·5H$_2$O**, and **1C**.

Table S1. Selected bond distances and angles of complexes **1P, 1P·5H$_2$O** compared to **1C**.

Table S2. Hydrogen-bonding O-H···O distances around the phosphonic acid groups of **1P·5H$_2$O**.

Figure S2. Intermolecular hydrogen bonds in the anhydrous form **1P**. The light green dotted lines show the intermolecular OH···N and OH···O hydrogen bonds.

Figure S3. Emission spectra of **1P·5H$_2$O**, **1P-H**, and **1P-V** in the solid state at 77 K.

Figure S4. Emission decays of **1P·5H$_2$O**, **1P-H** and **1P-V** at 298 K in the solid state.

Figure S5. Excitation and emission spectra of the aqueous solution of **1P**.

Figure S6. Changes of the emission spectra of **1P-V** and **1P-H** in the solid state under exposure to saturated water vapour at 293 K.

Figure S7. Water vapour adsorption isotherms of **1P-V** (blue squares) **1P-H** (red circles) at 298 K.

Figure S8. Temperature dependence of the PXRD pattern of **1P-V** (Cu Kα).

Figure S9. Thermogravimetric analyses for **1P·5H$_2$O**, **1P-V** and **1P-H**.

Figure S10. Magnified view of the ν(C≡N) region in IR spectra of **1P·5H$_2$O**, **1P-V** heated at 393 K, **1P-V** at 303 K after heating, and **1P-H**.

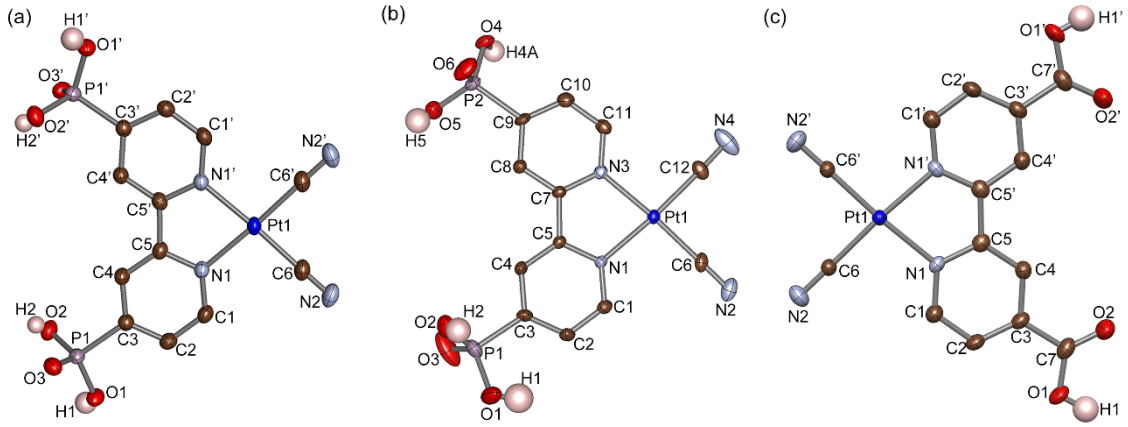

Figure S1. Molecular structures with the numbering schemes of complexes (a) **1P**, (b) **1P·5H$_2$O**, and (c) **1C**.

Table S1. Selected bond distances (Å) and angles (°) of complexes **1P, 1P·5H$_2$O** compared to **1C**.

	1P	**1P·5H$_2$O**		**1C**[a]
	200 K	200 K	80 K	200 K
Pt1-C6	1.951(3)	1.957(6)	1.958(5)	1.959(9)
Pt1-C12	-	1.965(6)	1.959(5)	-
Pt1-N1	2.049(2)	2.058(4)	2.055(4)	2.049(7)
Pt1-N3	-	2.052(4)	2.056(4)	-
N2-C6	1.152(4)	1.147(7)	1.153(7)	1.14 (1)
N4-C12	-	1.127(8)	1.148(7)	-
P1-O1	1.540(2)	1.538(5)	1.534(5)	-
P1-O2	1.553(2)	1.544(5)	1.540(5)	-
P1-O3	1.492(2)	1.491(6)	1.493(5)	-
P2-O4	-	1.547(4)	1.550(4)	-
P2-O5	-	1.516(5)	1.520(4)	-
P2-O6	-	1.499(5)	1.499(4)	-
Pt1-Pt1'	4.5937(1)	3.3775(9)	3.3488(7)	3.255(1)
Pt1-Pt1"	4.5937(1)	3.3700(9)	3.3403(7)	-
Pt1'-Pt1-Pt1"	146.735(6)	169.223(12)	169.103(12)	171.96(6)

[a]Ref. S1.

Table S2. Hydrogen-bonding O-H···O distances (Å) around the phosphonic acid groups of **1P·5H$_2$O** at 200 K.

Atom 1	Atom 2: A1-A2 distance	Atom 3:A1-A3 distance	A4: A1-A4 distance
O1	O5: 2.551(7)	-	-
O2	O10: 2.476(10)	-	-
O3	O8:2.653(10)	O10: 2.723(10)	O11:2.57(3)
O4	O7: 2.505(6)	-	-
O5	O1: 2.551(7)	O8: 2.580(11)	-
O6	O7: 2.675(8)	O9: 2.596(10)	-
O7	O4: 2.505(6)	O6: 2.675(8)	-
O8	O3: 2.653(10)	O5: 2.580(11)	O9: 2.502(12)
O9	O6: 2.596(10)	O8: 2.502(12)	
O10	O3: 2.723(10)	O11: 2.55(2)	-
O11	O3: 2.57(3)	O10: 2.55(2)	-

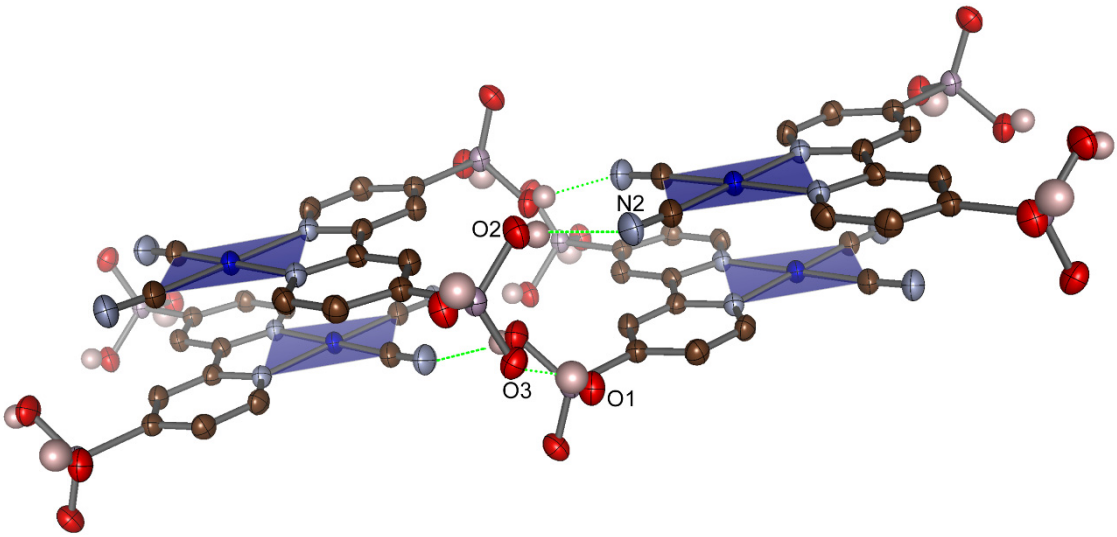

Figure S2. Intermolecular hydrogen bonds in the anhydrous form **1P**. The light green dotted lines show the intermolecular OH···N and OH···O hydrogen bonds.

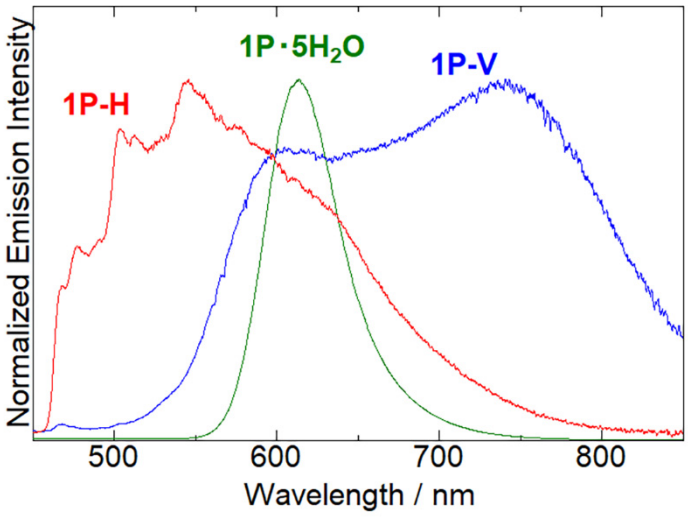

Figure S3. Emission spectra of **1P·5H$_2$O**, **1P-H**, and **1P-V** in the solid state at 77 K (λ_{ex} = 400 nm). The peak shoulder at around 610 nm observed for both **1P-H** and **1P-V** might be due to the *in-situ* generated **1P·5H$_2$O** in the cooling process.

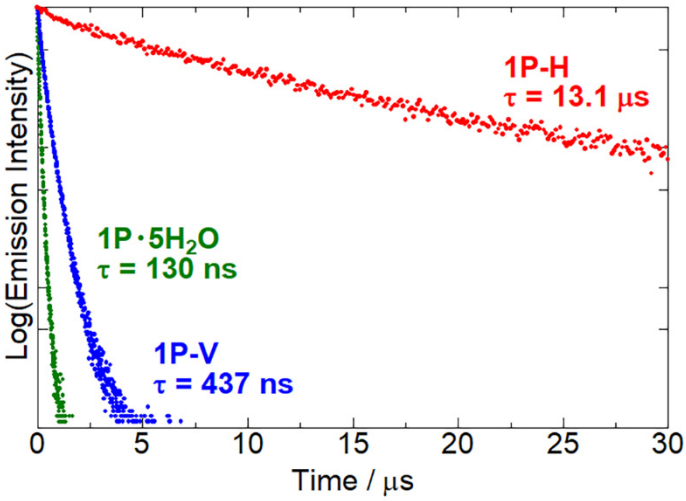

Figure S4. Emission decays of **1P·5H$_2$O** (green), **1P-H** (red) and **1P-V** (blue) at 298 K in the solid state (λ_{ex} = 280 nm).

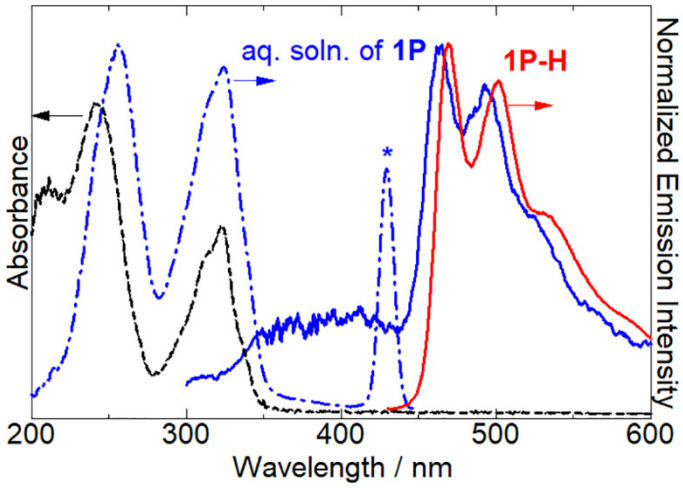

Figure S5. Excitation (blue chain line, λ_{em} = 500 nm) and emission spectra (blue solid line, λ_{ex} = 256 nm) of the aqueous solution of **1P** compared to the UV-Vis absorption spectrum of the same aqueous solution of **1P** (black dotted line) and the emission spectra of the heat-dried sample **1P-H** (red solid line, λ_{ex} = 400 nm). All spectra were measured at 293 K. The peak marked by asterisk (*) at 430 nm is derived from the Raman scattering of solvent water.

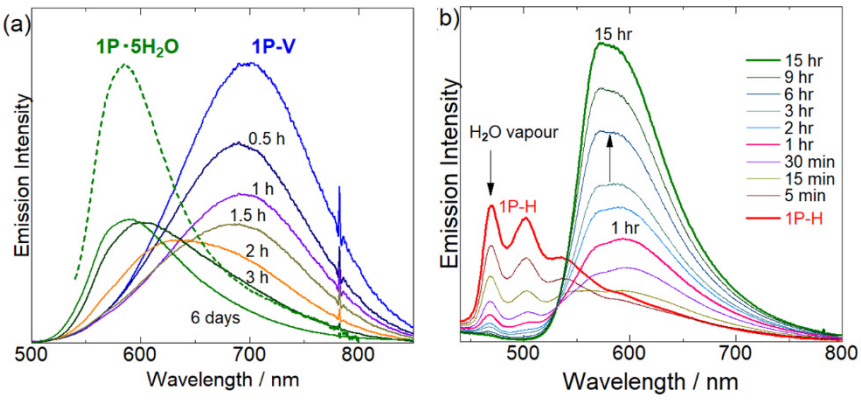

Figure S6. Changes of the emission spectra of (a) **1P-V** and (b) **1P-H** in the solid state under exposure to saturated water vapour at 293 K (λ_{ex} = 400 nm).

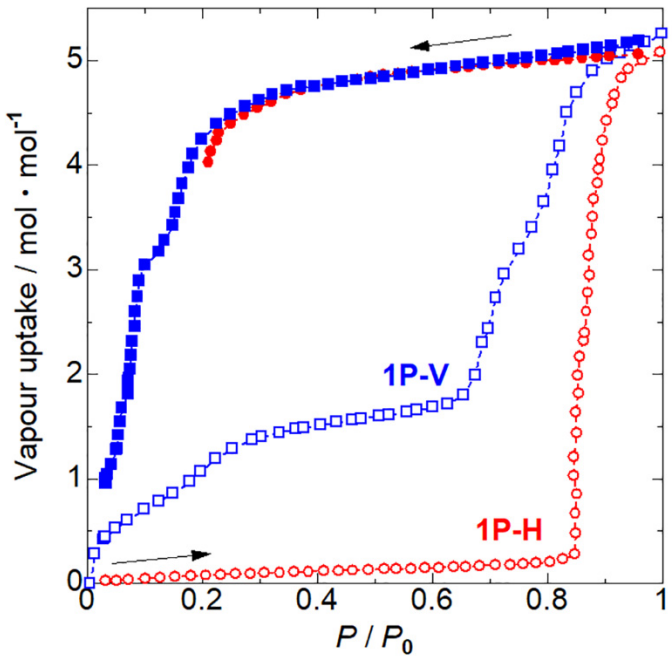

Figure S7. Water vapour adsorption isotherms of **1P-V** (blue squares) **1P-H** (red circles) at 298 K. Open and closed symbols show the adsorption and desorption processes. Each sample was dried at 393 K under vacuum for 12 hours.

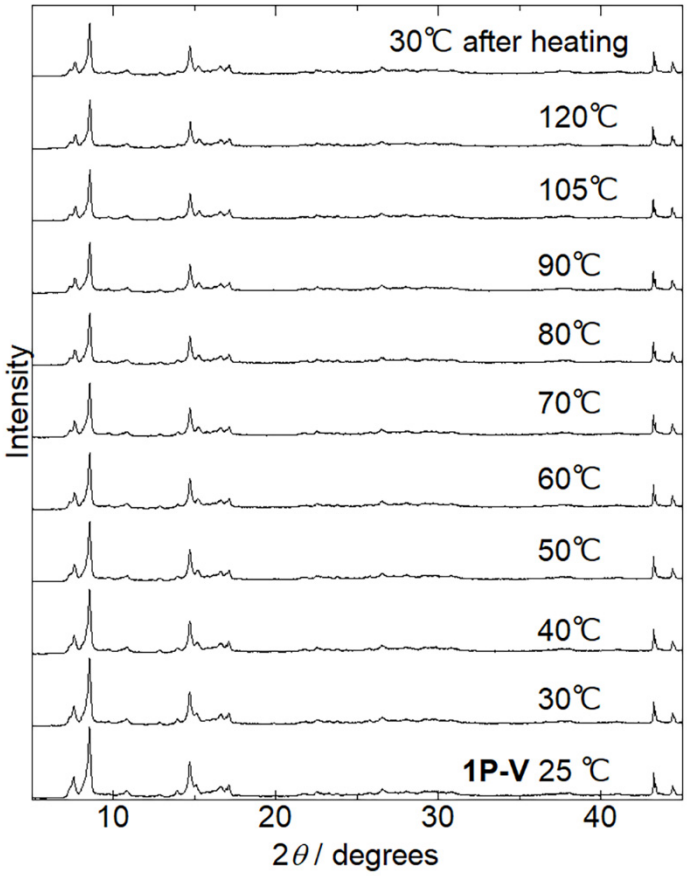

Figure S8. Temperature dependence of the PXRD pattern of **1P-V** (Cu Kα).

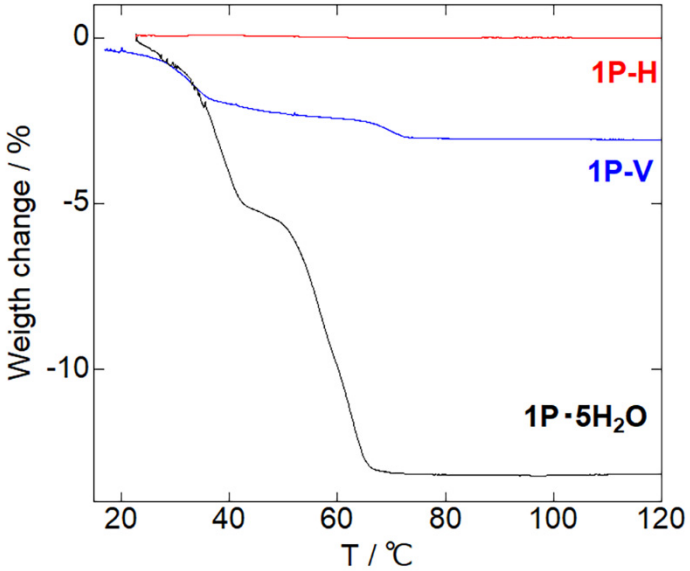

Figure S9. Thermogravimetric analyses for **1P·5H$_2$O** (black line), **1P-V** (blue line) and **1P-H** (red line) under Ar flow (300 mL/min). Observed weight losses at 100 °C (–13.3%, –3.0% and –0.18% for **1P·5H$_2$O**, **1P-V** and **1P-H**) are quantitatively agreed with the amount of hydrated water molecules in the three phases (13.7% for the *penta*-hydrated **1P·5H$_2$O**, 3.1% for *mono*-hydrated **1P-V** and 0 % for anhydrous **1P-H**).

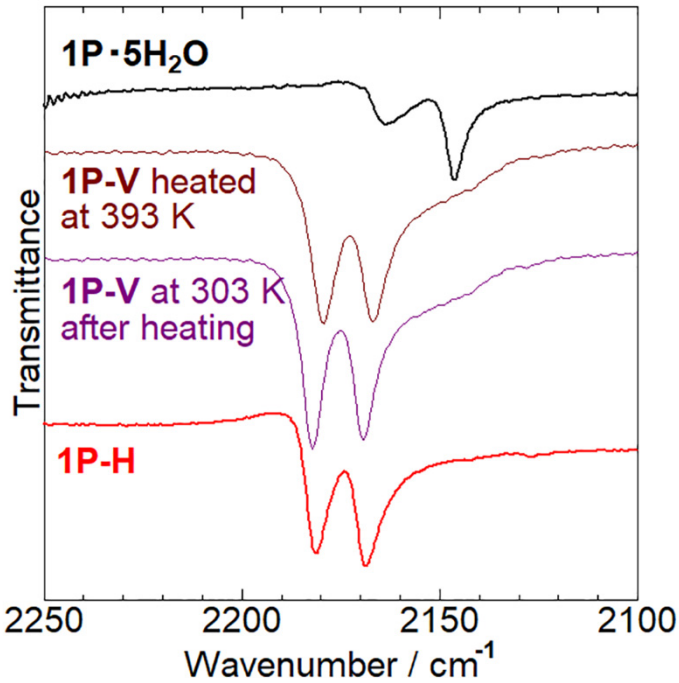

Figure S10. Magnified view of the ν(C≡N) region in IR spectra of **1P·5H$_2$O** (black line), **1P-V** heated at 393 K (brown line), **1P-V** at 303 K after heating (purple line), and **1P-H** (red line).

Reference

S1. Y. Shigeta, A. Kobayashi, T. Ohba, M. Yoshida, T. Matsumoto, H.-C. Chang, and M. Kato, *Chem. Eur. J.*, 2016, **22**, 2682-2690.